

Quantum corrections to the conductivity and quantum Hall effect in GaAs-GaAlAs multiple quantum well structures

V. A. Kulbachinskii and V. G. Kytin

Low Temperature Physics Department, Moscow Lomonosov University, 119899 Moscow, Russia

V. I. Kadushkin and E. L. Shangina

Technological Institute, Ryazin, Russia

A. de Visser

Van der Waals-Zeeman Laboratory, University of Amsterdam, Valckenierstraat 65, 1018 XE Amsterdam, The Netherlands

(Received 17 August 1993; accepted for publication 1 November 1993)

The magnetotransport properties of GaAs-GaAlAs multiple quantum well structures, with widths of the quantum wells $L_w = 33\text{--}66 \text{ \AA}$, have been investigated over a wide temperature and field range. The variation of the electron mobility with L_w (and temperature) can be accounted for by interface roughness scattering. A negative magnetoresistance was observed. An analysis within the theory of weak localization allowed us to evaluate the relaxation time of the phase of the electronic wave function and its temperature dependence $\tau_\varphi(T)$. Measurements in high-magnetic fields (up to 40 T) at $T = 4.2 \text{ K}$ revealed pronounced Shubnikov-de Haas oscillations and the quantum Hall effect.

I. INTRODUCTION

Artificial semiconductor superlattices are composed of a periodic sequence of crystalline layers of alternating composition (GaAs-GaAlAs) or of alternating doping (*n*-Si/*p*-Si), or of a combination of both (see, e.g., Ref. 1). The interest in artificial superlattices finds its origin in a one-dimensional periodic potential, induced by a periodic variation of either impurities or alloy composition, with a period shorter than the electron mean-free path. The predicted peculiarities of the optical and transport phenomena arise from a splitting of the conduction and valence bands into narrow minibands.

One of the important and suitable manners to grow artificial semiconductor superlattices is molecular beam epitaxy (MBE). The most famous structure consists of alternating layers of GaAs and $\text{Ga}_{1-x}\text{Al}_x\text{As}$ with x ranging from 0.15 to 0.35 and periods ranging from 50 to 250 \AA . By modulation doping in GaAs- $\text{Ga}_{1-x}\text{Al}_x\text{As}$ superlattices, their physical properties are considerably modified, and the interesting physical phenomena are extended to, e.g., quantum Hall effect (QHE) and quantum corrections to the conductivity.

In the past years the high sensitivity²⁻⁴ of GaAs- $\text{Ga}_{1-x}\text{Al}_x\text{As}$ superlattices and multiple quantum well (MQW) structures in the infrared spectral range 8–14 μm has attracted much attention. The physical properties of superlattices and MQW structures are governed by electron scattering processes. The electron mobility in superlattices may be connected with mechanisms like charge impurity scattering, interface roughness scattering, etc. The electron scattering mechanism may be investigated by optical or galvanomagnetic techniques. For instance, photoluminescence spectroscopy revealed that in doped superlattices the linewidth is large than in undoped superlattices. In this paper we report on a study of the galvanomagnetic properties of GaAs- $\text{Ga}_{1-x}\text{Al}_x\text{As}$ multiple quantum well

structures. The experiments have been carried out in the temperature interval $4.2 \text{ K} < T < 300 \text{ K}$ and in magnetic fields up to 40 T.

II. EXPERIMENT

GaAs- $\text{Ga}_{1-x}\text{Al}_x\text{As}$ MQW structures were grown by MBE. The sample structure is shown schematically in Fig. 1. Fifty periodic layers of GaAs (width $L_w = 33\text{--}66 \text{ \AA}$) and $\text{Ga}_{1-x}\text{Al}_x\text{As}$ ($x = 0.3$, width 254 \AA) were prepared. The quantum wells were doped with Si up to a concentration of $2 \times 10^{18} \text{ cm}^{-3}$. The structure was separated from a GaAs(Cr) substrate by an *i*- $\text{Ga}_{1-x}\text{Al}_x\text{As}$ buffer (width 1 μm). All structures were covered by a contact layer of *n*-GaAs (width 200 \AA). Double Hall bridges (channel width 150 μm) were prepared for measurements in a magnetic field.

The conductivity was measured in the temperature interval 4.2–300 K, and the Hall effect and the magnetoresistance were measured in the temperature interval 4.2–100 K, using standard techniques. Magnetic fields up to 6 T were produced by a superconducting solenoid. A part of the experiments have been performed in the High Field Magnet of the University of Amsterdam.⁵ This long-pulse magnet is capable of reaching fields up to 40 T with a total pulse duration of 1 s.

III. RESULTS

Samples with different well widths (L_w) were investigated. In Table I we have listed some typical parameters of the measured samples (labeled No. 1, No. 2, and No. 3). Note that the electron concentration (n) is given per quantum well. The conducting layer (*n*-GaAs, width 200 \AA) was excluded in the calculations. The semiwidth of the photoluminescence peak (δE) at $T = 4.2 \text{ K}$ amounts to 15–21 meV for the doped and to 4–5 meV for the undoped structures with identical geometrical parameters.

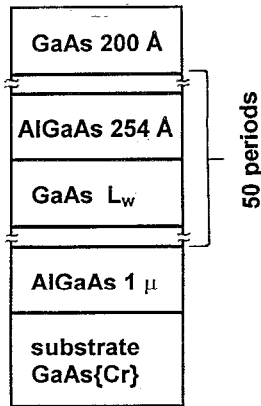


FIG. 1. Schematic structure of the GaAs-Ga_{1-x}Al_xAs samples ($x=0.3$). The well width L_w varies between 33 and 66 Å.

The temperature variation of the sheet conductivity $\sigma_{\square}(T)$ per quantum well is shown in Fig. 2. For all the samples the conductivity decreases with decreasing temperature. For $T < 20$ K $\sigma_{\square}(T) \propto \ln T$. The electron mobility (μ) increases for increasing L_w (see Table I).

The transverse magnetoresistance (ρ_{xx}) is negative at low temperatures ($B < 6$ T). It has the following characteristics: (i) $\rho_{xx} \propto B^2$ up to ~ 0.1 T, (ii) the field range of the B^2 dependence is reduced by decreasing the temperature, and (iii) for fields larger than 0.4, 0.2, and 0.06 T for samples No. 1, No. 2, and No. 3, respectively, we find $\rho_{xx} \propto \ln B$, up to the maximal field value (6 T). In Fig. 3 we show the relative change of the conductivity with field, $[\sigma(B) - \sigma(0)]/\sigma(0)$, plotted versus $\ln B$, at different temperatures. For $T > 150$ –200 K the magnetoresistance becomes positive and varies as B^2 .

Hall-effect measurements showed that the electron concentration is independent of temperature for all three samples (see Fig. 4). This implies that $\sigma(T)$ is dominated by $\mu(T)$. The variation of μ with temperature is shown in Fig. 5.

In spite of the low mobilities of our samples we observed the QHE, albeit in very high-magnetic fields. In Figs. 6 and 7 we show the transverse magnetoresistance $\rho_{xx}(B)$ and the Hall resistance $\rho_{xy}(B)$ at $T=4.2$ K for two samples (No. 1 and No. 3). From these figures it can be concluded that all the parallel connected quantum wells exhibit almost the same electron density in the populated ground subband, which results in one observable period of Shubnikov-de Haas (SdH) oscillations. The ρ_{xy} plateaus,

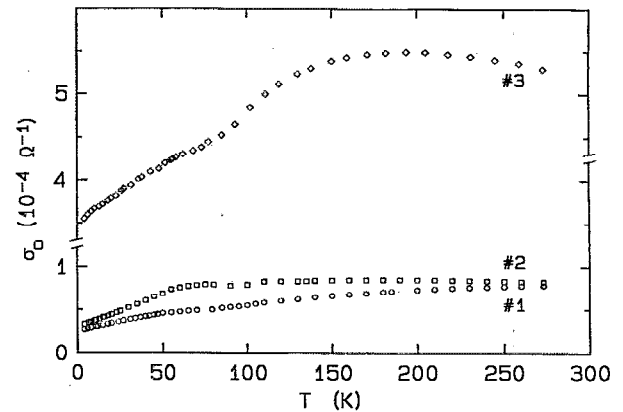


FIG. 2. Sheet conductivity vs temperature for samples No. 1 (○), No. 2 (□), and No. 3 (◇).

which are most sensitive to inhomogeneities, show only weak additional structures in the case of sample No. 3. The electron concentration evaluated from the SdH signal is almost the same as the one calculated from the Hall effect.

IV. ANALYSIS AND DISCUSSION

The electron mobility μ of the studied samples rapidly decreases when the width of the quantum well decreases. In Fig. 8 we show the dependence of μ on L_w in a double logarithmic plot. Our data are in good agreement with the results obtained in Ref. 6. In Ref. 7 it was proposed that in thin quantum wells ($L_w < 60$ Å) interface roughness scattering is the dominant scattering mechanism. In that case the electron mobility is proportional to L_w^6 and depends on the lateral roughness width Λ and height Δ in the following way:

$$\mu = \frac{L_w^6}{\Delta^2 \Lambda^2} g(\Lambda, n, T), \quad (1)$$

where $g(\Lambda, n, T)$ is a smooth function of temperature T , electron concentration n , and the parameter Λ . We have evaluated $\mu(T)$ for the cases of dominant charge impurity scattering (because the quantum wells are doped) and dominant interface roughness scattering. The effect of impurity scattering has been calculated using the equations of Ref. 8. However, the calculated mobilities are about one order of magnitude higher than the experimental values and moreover exhibit a different temperature dependence. In order to calculate the effect of the second mechanism we

TABLE I. Well width (L_w), Fermi energy (E_F), electron concentration per well (n), coefficient of diffusion (D), mobility (μ), semiwidth of the photoluminescence peak (δE), and fluctuation energy of the ground-state in the quantum well (δE_0) for samples No. 1, No. 2, and No. 3 at $T=4.2$ K.

No.	L_w (Å)	E_F (meV)	n (10^{11} cm ⁻²)	μ (cm ² /V s)	D (cm ² /s)	δE (meV)	δE_0 (meV)
1	33	23	6.5	260	7.2	21	30
2	44	15	4.3	480	8.8	13	16
3	66	92	25.7	860	47	15	7

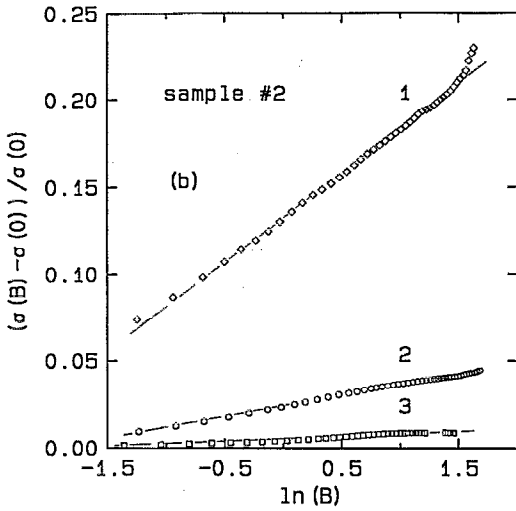
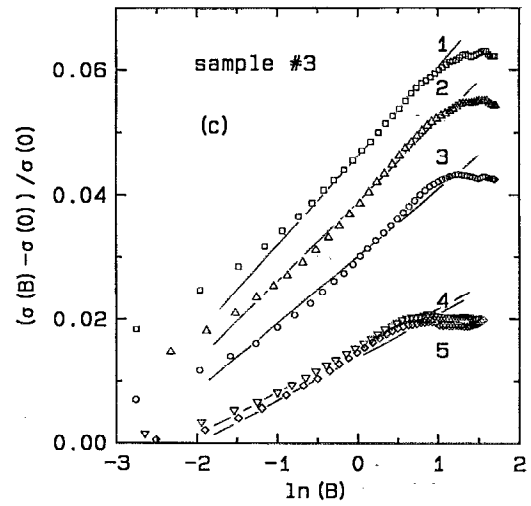
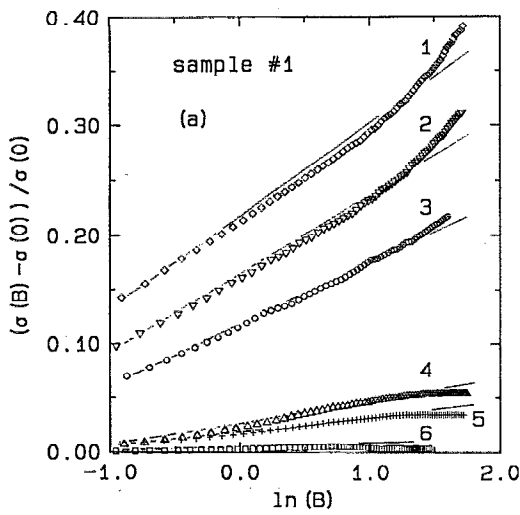


FIG. 3. Relative change of the conductivity versus magnetic field (on a logarithmic scale). (a) Sample No. 1 at (1) 4.2 K, (2) 5.5 K, (3) 10.6 K, (4) 51.5 K, (5) 81.5 K, and (6) 138 K. (b) Sample No. 2 at (1) 4.2 K, (2) 20.2 K, and (3) 51.8 K. (c) Sample No. 3 at (1) 4.2 K, (2) 9.3 K, (3) 20.5 K, (4) 43 K, and (5) 69.5 K. The solid lines represent fits to Eq. (3).

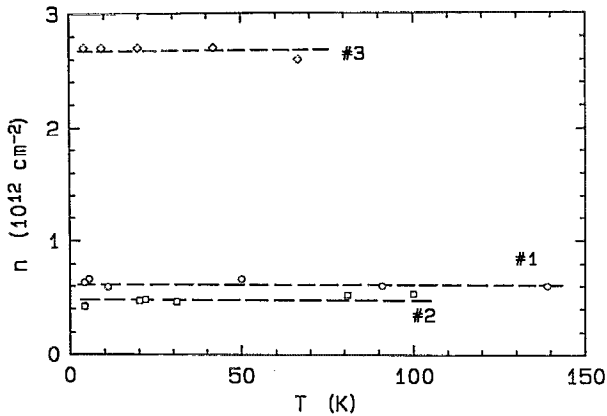


FIG. 4. Electron concentration per well vs temperature for samples No. 1 (\circ), No. 2 (\square), and No. 3 (\diamond). Dashed lines are a guide to the eye.

used Eq. (1) and compared the theoretical curves to the data points using Δ and Λ as fitting parameters. The results of this fitting procedure are shown in Fig. 8 for samples No. 1 and No. 2. Good agreement is observed for Δ equal to 2.83 Å, while Λ equals 130 and 100 Å for samples No. 1 and No. 2, respectively. For sample No. 3 the fitting procedure is not adequate, which suggests that it is necessary to take into account also impurity scattering. However, this is a much more complicated task. Recently, also for AlAs/GaAs quantum wells the observed variation of μ with temperature was attributed to a dominant interface roughness scattering mechanism.⁹

Having established the temperature and field dependence of the conductivity of our samples (Figs. 2 and 3), we next are able to determine some electronic parameters of the samples, e.g., the relaxation time of the phase of the electron wave function, τ_ϕ . The value of τ_ϕ depends on electron-electron and/or electron-phonon relaxation. The relationship between τ_ϕ and the other characteristic times such as the average time between inelastic collisions (τ_{in})

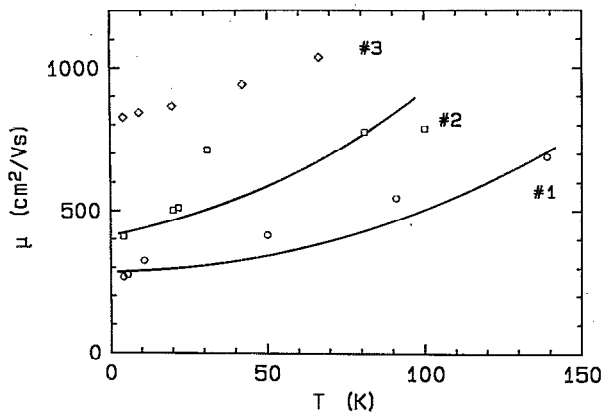


FIG. 5. Mobility vs temperature for samples No. 1 (○), No. 2 (□), and No. 3 (◇). The solid lines represent $\mu(T)$ calculated with Eq. (1), with parameters $\Lambda=130 \text{ \AA}$ and $\Delta=2.83 \text{ \AA}$ for sample No. 1, and $\Lambda=100 \text{ \AA}$ and $\Delta=2.83 \text{ \AA}$ for sample No. 2.

and the energy relaxation time (τ_e) was calculated in Refs. 10 and 11.

The experimental results, i.e., the decrease of $\sigma(T)$ with decreasing temperature and the negative magnetoresistance, which varies as B^2 in the low-field range and as $\ln B$ in the high-field range, may be fully described by the theory of quantum corrections to the conductivity for the two-dimensional (2D) case,^{12,13} which is valid for $k_B T \ll E_f$.

The conductivity $\Delta\sigma(T)$ in zero magnetic field of 2D disordered systems, due to weak localization and electron-electron interaction effects, is given by^{10,11}

$$\begin{aligned} \Delta\sigma(T) &= \sigma(T_2) - \sigma(T_1) \\ &= [\beta + p(1-\beta) + \gamma] \frac{e^2}{2\pi^2\hbar} \ln\left(\frac{T_2}{T_1}\right), \end{aligned} \quad (2)$$

where p is the exponent of the temperature dependence of τ_φ , which is expressed as

$$\tau_\varphi = aT^{-p}. \quad (3)$$

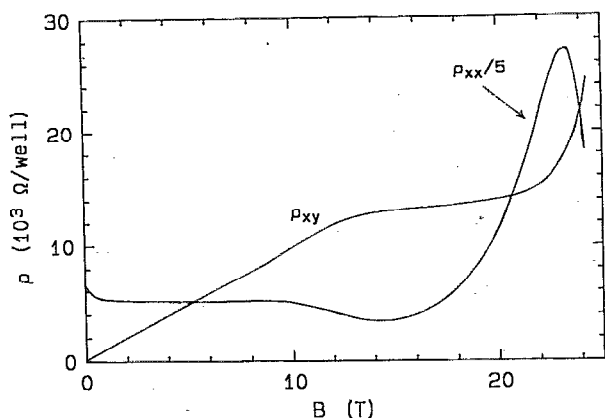


FIG. 6. Shubnikov-de Haas oscillations (ρ_{xx}) and quantum Hall effect (ρ_{xy}) at $T=4.2 \text{ K}$ for sample No. 1.

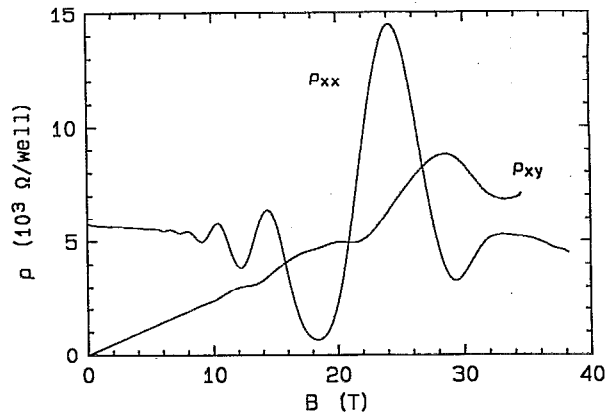


FIG. 7. Shubnikov-de Haas oscillations (ρ_{xx}) and quantum Hall effect (ρ_{xy}) at $T=4.2 \text{ K}$ for sample No. 3.

For electron-electron interaction in weakly disordered metals it was found that $p=d/2$, in contrast with the result $p=2$ predicted for the clean limit whatever the dimensionality of the system is. For electron-phonon scattering p ranges between 2 and 4 in the dirty limit at low temperatures. The coefficient β represents the Maki-Thompson correction to the conductivity. The strength of the electron-electron interaction contribution is given by γ , where γ which is a measure of the screening by other charge carriers, has a value close to 1 in the limit of weak screening.

The correction to the sheet conductivity σ_\square in a magnetic field B has the form¹²

$$\sigma(B) - \sigma(0) = \frac{e^2}{2\pi^2\hbar} (1-\beta) f_2 \left(\frac{4DBe\tau_\varphi}{\mu_0\hbar c} \right), \quad (4)$$

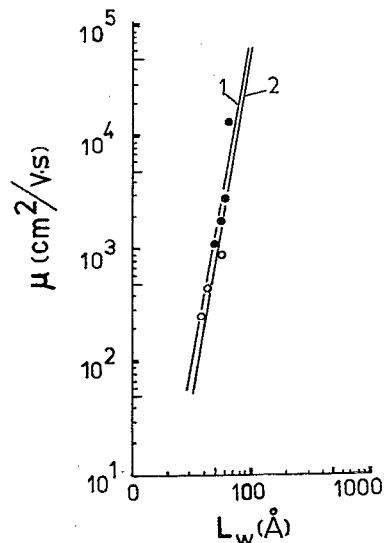


FIG. 8. Mobility vs well width on a double logarithmic scale. Open circles from this work and closed circles from Ref. 6. The solid lines correspond to calculations with the lateral roughness width (1) $\Lambda=50 \text{ \AA}$ and (2) $\Lambda=70 \text{ \AA}$ (after Ref. 7).

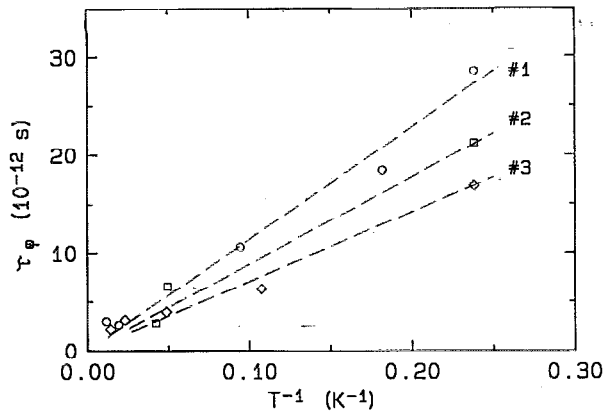


FIG. 9. Relaxation time of the phase of the electron wave function vs $1/T$ for samples No. 1 (○), No. 2 (□), and No. 3 (◇).

where the function f_2 describes the localization and D is the carrier diffusion coefficient. For $x \ll 1$ $f_2(x) \approx x^2/24$ and for $x \gg 1$ $f_2(x) \approx \ln(x)$. According to Refs. 14 and 15, Eq. (4) is valid only when the magnetic length $l_B = (\hbar c \mu_0 / e B)^{1/2}$ is larger than the mean-free path l . For the investigated samples with a mobility $\mu < 860 \text{ cm}^2/\text{V s}$ it is possible to use Eq. (4) in the applied field range. The magnetic field dependence of γ is significant only in high-magnetic fields ($g\mu_B B / k_B T > 1$) and at low temperatures, and hence is neglected. Making use of the relation

$$\mu = \frac{eD}{E_F}, \quad (5)$$

we obtain the values of D for the degenerate electron gas as listed in Table I. Using τ_φ as a fitting parameter in Eq. (4), we next compare the theoretical curves to the experimental negative magnetoresistance (see Fig. 2, solid lines). The values of τ_φ evaluated from this fitting procedure are plotted versus reciprocal temperature in Fig. 9. The linear dependence of τ_φ on $1/T$ reveals that Eq. (3) is obeyed for $p=1$. This value of p corresponds to dominant electron-electron interaction in the 2D MQW structures.

V. CONCLUSIONS

Magnetotransport measurements of GaAs-GaAlAs multiple quantum well structures have been performed over a wide temperature and field range. By analyzing the data within the existing theoretical frameworks a number of interesting conclusions can be drawn. In narrow quantum wells ($L_w = 33\text{--}66 \text{ \AA}$) interface roughness scattering is the dominant scattering mechanism, even in the case of doped quantum wells. Quantum corrections to the conductivity for the 2D case play an important role in the explanation of the magnetotransport properties of the MQW structures. The experimental results indicate a strong electron-electron interaction. Besides, the QHE was observed in high-magnetic fields for very low mobility samples. The QHE reveals that all the parallel connected quantum wells exhibit almost the same electron density in the populated ground subbands. The ρ_{xy} plateaus, which are very sensitive to inhomogeneities, show only weak additional structures.

¹K. Ploog and G. H. Döhler, *Adv. Phys.* **32**, 285 (1983).

²B. F. Levine, C. G. Bethea, G. Hasnain, J. Walker, and R. J. Malik, *Appl. Phys. Lett.* **53**, 296 (1988).

³G. Hasnain, B. F. Levine, C. G. Bethea, R. A. Logan, J. Walker, and R. J. Malik, *Appl. Phys. Lett.* **54**, 2515 (1989).

⁴B. F. Levine, G. Hasnain, C. G. Bethea, and N. Chand, *Appl. Phys. Lett.* **54**, 2704 (1989).

⁵R. Gersdorf, F. R. de Boer, J. C. Wolfart, F. A. Müller, and L. W. Roeland, in *High Field Magnetism*, edited by M. Date (North-Holland, Amsterdam, 1983), p. 277.

⁶K. Hirakawa, T. Noda, and H. Sakaki, *Surf. Sci.* **196**, 365 (1988).

⁷H. Sakaki, T. Noda, K. Hirakawa, M. Tanaka, and T. Matsusue, *Appl. Phys. Lett.* **51**, 1934 (1987).

⁸A. Ando, A. Fauler, and F. Stern, *Rev. Mod. Phys.* **54**, 437 (1982).

⁹T. Noda, M. Tanaka, and H. Sakaki, *Appl. Phys. Lett.* **57**, 1651 (1990).

¹⁰B. L. Al'tshuler and A. G. Aronov, in *Modern Problems in Condensed Matter Science*, edited by A. L. Efros and M. Pollak (North-Holland, Amsterdam, 1985), p. 1.

¹¹A. G. Aronov, *Physica B* **126**, 314 (1984).

¹²B. L. Al'tshuler, A. G. Aronov, A. N. Larkin, and D. E. Khmel'nitskii, *Sov. Phys. JETP* **54**, 411 (1981).

¹³E. Abrahams, P. W. Anderson, D. C. Licciardello, and T. V. Ramakrishnan, *Phys. Rev. Lett.* **42**, 673 (1979).

¹⁴B. L. Al'tshuler, A. G. Aronov, and D. E. Khmel'nitskii, *J. Phys. C* **15**, 7367 (1982).

¹⁵T. A. Polyanskaya and Y. V. Shmartsev, *Sov. Phys. Semicond.* **23**, 1 (1988).